Intelligent Local Area Signals Based Damping of Power System Oscillations Using Virtual Generators and Approximate Dynamic Programming

Diogenes Molina, *Student Member, IEEE*, Ganesh Kumar Venayagamoorthy, *Senior Member, IEEE*, Jiaqi Liang, *Member, IEEE*, and Ronald G. Harley, *Fellow, IEEE*

***Abstract*—This paper illustrates the development of an intelligent local area signals based controller for damping low-frequency oscillations in power systems. The controller is trained offline to perform well under a wide variety of power system operating points, allowing it to handle the complex, stochastic, and time-varying nature of power systems. Neural network based system identification eliminates the need to develop accurate models from first principles for control design, resulting in a methodology that is completely data driven. The virtual generator concept is used to generate simplified representations of the power system online using time-synchronized signals from phasor measurement units at generating stations within an area of the system. These representations improve scalability by reducing the complexity of the system "seen" by the controller and by allowing it to treat a group of several synchronous machines at distant locations from each other as a single unit for damping control purposes. A reinforcement learning mechanism for approximate dynamic programming allows the controller to approach optimality as it gains experience through interactions with simulations of the system. Results obtained on the 68-bus New England/New York benchmark system demonstrate the effectiveness of the method in damping low-frequency inter-area oscillations without additional control effort.**

***Index Terms*—Approximate dynamic programming, generator coherency, inter-area oscillations, power system equivalents, power system stabilizer, virtual generator.**

I. Introduction

POWER systems are being pushed to operate closer to their stability limits. This trend is caused by increasing electrical energy demands coupled with limited investment in transmission infrastructure and energy market deregulation. One of the manifestations of this stability reduction is the emergence or worsening of low-frequency oscillations. Some power systems report a noticeable increase in the number of events involving these oscillations [1]. In general, power system oscillations are mitigated (or damped) using power system stabilizers (PSSs). A PSS injects a supplementary signal to the excitation system of the synchronous generator it is connected to [2]. This supplementary signal is generated using only local measurements, which limits its effectiveness for system-wide damping control.

It is not clear that the conventional damping control approach using local PSSs will be effective enough to damp low-frequency oscillations [3]. However, the advent of phasor measurement units (PMUs) and advanced communication infrastructures has opened the door to improved damping control algorithms due to the availability of time-synchronized signals from different locations in the system. It has been shown that controllers that make use of these signals could damp power system oscillations more effectively than conventional local controllers [3], [4].

The work in [5] presents a decentralized/hierarchical approach for the coordinated design of PSSs that make use of wide-area signals to improve the damping of low-frequency oscillations in the Hydro-Quebec system. The approach relies on linear system identification and control design techniques, and therefore the performance of the resulting controllers is likely to degrade as the system's operating point shifts away from that used for controller design. An approach to deal with this issue can be found in [6], where the controllers are developed using a linearized model of the power system and robust control techniques. The resulting controllers were then tuned using the full non-linear model of the system to ensure appropriate performance. A neural network (NN) based method for dealing with the non-linear and time-varying nature of power systems is presented in [7]. Appropriate offline training of these controllers ensures robustness and allows them to maintain their level of performance even as the operating conditions of the power system change. However, as the size of the system grows, the computational requirements for achieving acceptable performance from NNs can become prohibitive. This poor scalability can make these controllers impractical for realistically sized systems [8].

A method for designing a scalable intelligent local-area signals based damping controller for power systems is presented in this paper. The terms "local area signals based" highlight that input and output locations are limited to a relatively small portion of the system: the "local area". However, the control objective is to damp oscillations associated with inter-area modes. The method results from the combination of the virtual

Manuscript received May 30, 2012; revised October 08, 2012; accepted November 28, 2012. Date of publication February 08, 2013; date of current version February 27, 2013. This work was supported by the U.S. National Science Foundation, under Grant EFRI #1238097. Any opinions, findings, and conclusions or recommendations expressed in this work are those of the authors and do not reflect the views of the National Science Foundation. Paper no. TSG-00315-2012.

D. Molina is with the School of Electrical and Computer Engineering, Georgia Institute of Technology, Atlanta, GA 30332 USA (e-mail: ddmolina@gatech.edu).

G. K. Venayagamoorthy is with the Holcombe Department of Electrical and Computer Engineering, Clemson University, Clemson, SC 29634 USA (e-mail: gkumar@ieee.org).

J. Liang is with ABB US Corporate Research Center, Raleigh, NC 27606 USA (e-mail: jiaqi.liang@us.abb.com).

R. G. Harley is with the School of Electrical and Computer Engineering, Georgia Institute of Technology, Atlanta, GA 30332 and also Professor Emeritus and an Honorary Research Associate at the University of KwaZulu-Natal, Durban, South Africa (e-mail: rharley@gatech.edu).

Color versions of one or more of the figures in this paper are available online at http://ieeexplore.ieee.org.

Digital Object Identifier 10.1109/TSG.2012.2233224

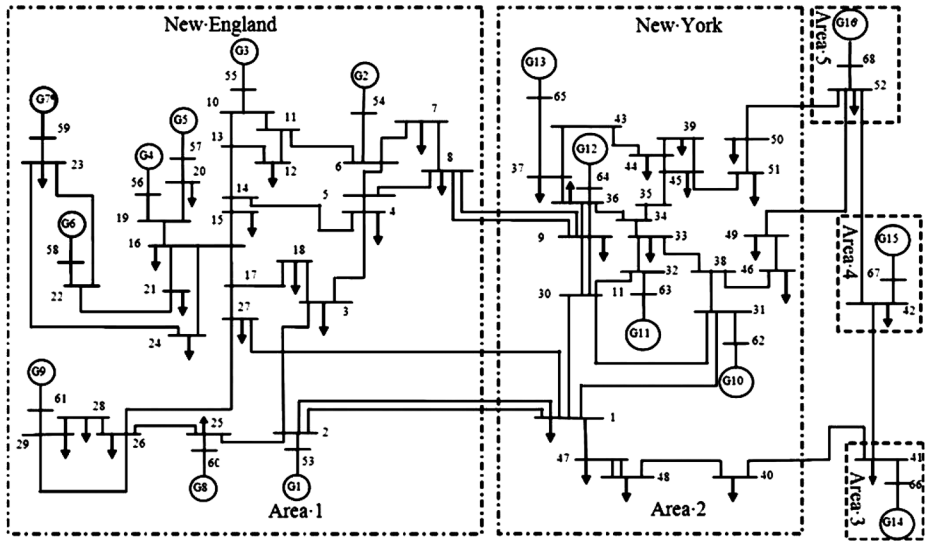

Fig. 1. Single line diagram of the 68-bus New England/New York power system.

generator (VG) concept [9], [10], coupled with NN-based non-linear dynamical system identification, and approximate dynamic programming. The end result is a controller that progressively improves its own performance and approaches optimality as it gains experience through interactions with power system simulations. Robustness is achieved by training the controller offline to perform well under a wide variety of operating points. The use of the virtual generator concept improves scalability and makes intelligent damping control more attractive for deployment in realistically sized systems. Simulations on a 68-bus system show that substantial improvements can be achieved without additional control effort compared to more conventional damping controllers.

The rest of the paper is organized as follows: Section II briefly describes the 68-bus power system used for evaluating the concepts outlined in the rest of the paper. Section III provides some basic concepts regarding generator coherency, describes the VG representations, and applies the VG to a portion of the 68-bus system. Section IV demonstrates how NN-based system identification techniques can be used to find an approximate input/output mapping of the VG dynamic behavior, and how the sensitivity of the VG speed to the local-area input points into the power system can be estimated from that mapping. Section V provides a brief description of heuristic dynamic programming, a reinforcement learning mechanism that finds approximate solutions of the Bellman equation of dynamic programming that can be used for intelligent adaptation of controller parameters. The details of the implementation of this methodology for adaptation of the intelligent local area signals based damping controller (ILADC) are also provided in this section. Section VI illustrates the effectiveness of the resulting ILADC for improving the stability of the 68-bus system by comparing against conventional PSSs. Section VII provides an insight into some of the issues that need to be addressed prior to implementing the ILADC in real power systems and points to potential solutions. Section VIII concludes the paper.

II. The 68-Bus New England/New York Power System

The power system in Fig. 1 represents a reduced order model of the New England/New York interconnection of more than 30 years ago. More details on the parameters of this model can be found in [11]. The automatic voltage regulator (AVR)/exciter and turbine/governor models for each generator are shown in Fig. 2. The AVR has two supplementary signal input points (u_{PSS}, and u_{LADC}). When connected, these inputs correspond to the output of a local PSS and/or of a local area damping controller (LADC) respectively. Generators G14–G16 represent large groups of generators and are equipped with PSSs. Each generator is simulated using 6th order synchronous machine models available in DIgSILENT PowerFactory, the network is represented by a set of algebraic equations, and the loads are represented as constant impedances.

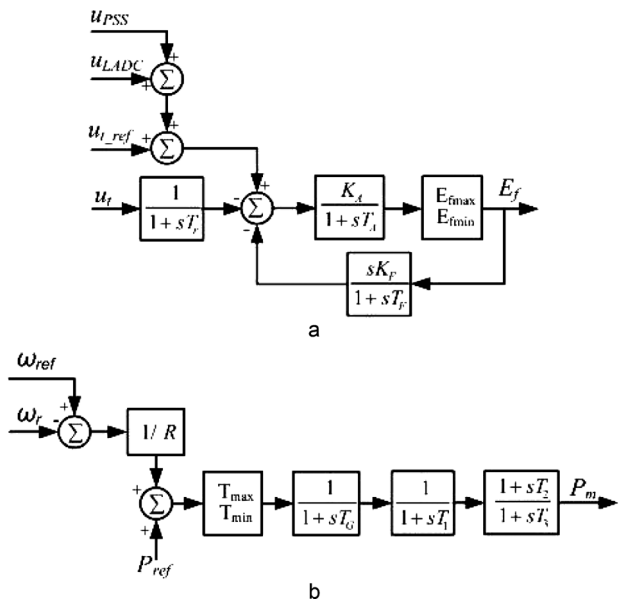

Fig. 2. Models of generator controls. (a) Automatic voltage regulator and exciter. (b) Turbine and governor.

For the purposes of this paper, only the New England side of the system is considered accessible; i.e., measurements and control inputs are only available for this portion of the system. This accounts for the fact that, in a real power system application, it is unlikely that a single entity would have access to the information/measurements of the entire power system.

III. Generator Coherency and Virtual Generators

The VG representation introduced in [9] relies on the concept of coherency. Coherency in power systems refers to the tendency of groups of generators to oscillate in phase at the same angular speed and maintaining the same rotor angle deviation. In [12], [13] it was demonstrated that, for certain kinds of power system studies, coherent behavior can be exploited to generate simplified dynamic equivalents of portions of power systems while maintaining acceptable simulation accuracy.

One of the methods for creating such simplified power system representations is called slow coherency aggregation [14]. The idea is to define the center of angle of a group of coherent machines as a slow variable, and their inter-machine oscillations as a fast variable. The definitions of these variables for a group of say 2 machines, for example, are shown in (1) and (2).

$$\delta_{slow} = \frac{H_1\delta_1 + H_2\delta_2}{H_1 + H_2} \tag{1}$$

$$\delta_{fast} = \delta_1 - \delta_2 \tag{2}$$

The constant H_i is the per unit inertia of generator i with all generators in the group referred to the same power base. Equation (1) can be differentiated to obtain:

$$\dot{\delta}_{slow} = \frac{H_1\dot{\delta}_1 + H_2\dot{\delta}_2}{H_1 + H_2} = \omega_{slow} = \frac{H_1\omega_1 + H_2\omega_2}{H_1 + H_2} \tag{3}$$

Generalizing for groups of N coherent generators results in:

$$\omega_{slow} = \frac{\sum_{i=1}^{N}(H_i\omega_i)}{\sum_{i=1}^{N}(H_i)} \tag{4}$$

The coherency assumption results in the vanishing of the fast variable in (2) to a small value that is neglected. Also, the availability of PMU data allows the real-time calculation of (4) as the system operates. As a consequence, large portions of the system containing a number of coherent generators can be represented as a single generator for local-area damping control purposes. The resulting "equivalent" generator is called a "virtual generator" (VG) from now onwards and its speed is given by (5)

$$\omega_{VG} = \omega_{slow} \tag{5}$$

An issue with this representation is that the validity of the coherency assumption, and consequently the validity of the VG representation, varies with the system operating condition and with the type of disturbance as shown in Section III-C.

A. Illustration of Coherency Determination

The VG concept assumes that the machines being represented are coherent. The method used to identify coherency is called FSHC and its details can be found in [9]. Three-phase faults are applied at a number of locations across the system to generate the swing curves. These curves are then grouped by similarity using hierarchical clustering algorithms available in MATLAB. The clustering results are summarized in the dendrogram shown in Fig. 3. The height of the horizontal links connecting one generator to another is a measure of the dissimilarity between the swing curves. None of the generators exhibit perfect coherency; however, 4 groups of coherent generators can be formed by selecting the coherency threshold line shown in the figure: {1, 8}, {2, 3}, {4, 5, 6, 7}, and {9}.

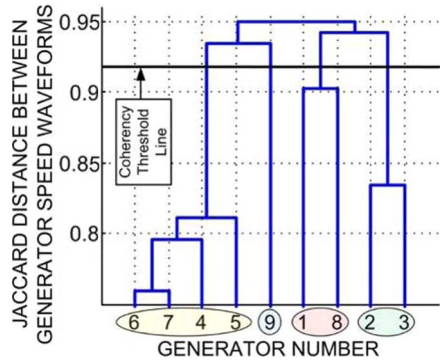

Fig. 3. Coherent generator clustering dendrogram.

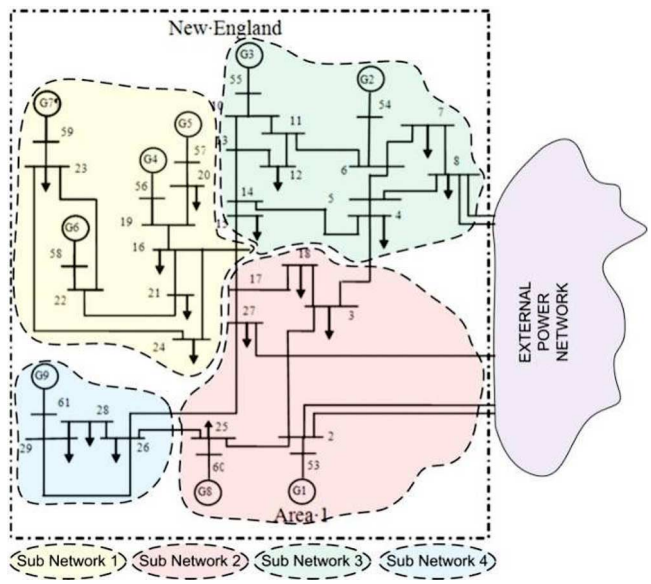

Fig. 4. Partitioning of the New England side of the 68-bus system.

B. Virtual Generators for the 68-Bus System

Complementing the information provided by Fig. 3 with load flow studies allows the partitioning of the 68-bus network into the four subnetworks shown in Fig. 4. The New York side of the system is now shown as an external power network that cannot be measured nor controlled.

For LADC, the rotor speeds of the generators inside of these subnetworks can be represented using one VG per subnetwork. Applying (5) to calculate the speeds of the four VGs after a disturbance in the system results in the waveforms shown in Fig. 5, and the subnetworks clearly respond in very different ways.

The simplifications performed so far are a way of interpreting information and measurements about the system; but, the actual system remains unchanged.

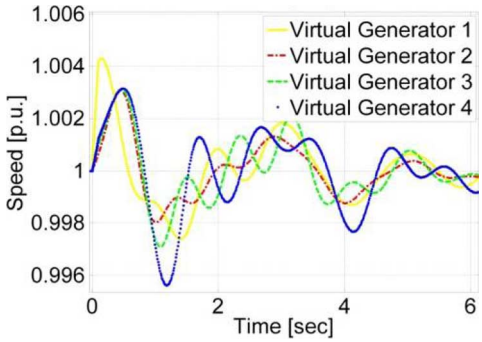

Fig. 5. VG speeds after a 3-phase short circuit disturbance.

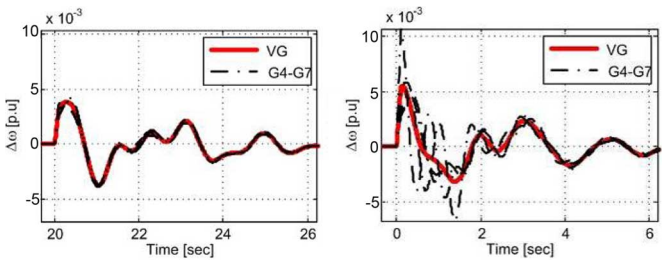

Fig. 6. Speed deviations for disturbance applied electrically far away (left) and close by (right).

C. Grouped Generators Don't Always Behave Coherently

The VG representation is based on the assumption that all generators in a group behave coherently. However, this assumption is typically satisfied only for disturbances that occur electrically far away from the coherent group. Fig. 6 (left) shows the speed deviations of generators G4–G7 and of the VG representing these four generators when a disturbance is applied at a remote location. The speeds of the generators are nearly identical, and the coherency assumption holds. In contrast, when the disturbance is applied electrically close by, the coherency assumption is violated, and the VG representation is no longer accurate as illustrated in Fig. 6 (right) for the same subnetwork. Nevertheless, simulation results will show that good damping can be achieved by the ILADC even when coherency is not fully satisfied.

IV. Identification of Virtual Generator Dynamics

The previous section described the VG concept and showed that groups of several coherent generators in a power system can be represented by a single VG speed. However, knowledge of the dynamical behavior of the VG is critical for the controller adaptation methodology presented in the next section.

The fact that the VG is not a real device in the system, but merely a way of interpreting local-area information from PMUs, makes developing an analytical model from first principles difficult at best. The neural network of this section provides an effective tool for finding a dynamical model of the VG using input/output data. This network is referred to as the model network.

A. Recurrent Neural Networks Based VG Model

Proven universal approximation capabilities coupled with the availability of effective parameter adaptation (training) algorithms make NNs good candidates for non-linear dynamical system identification [15]. The neuro-identification task is illustrated in Fig. 7 and can be summarized as: given the present

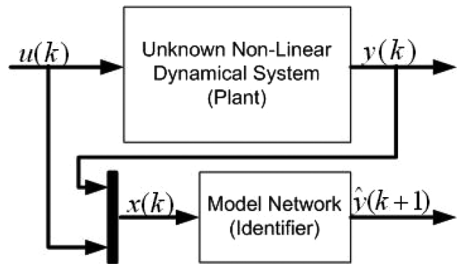

Fig. 7. Configuration for neural network based system identification.

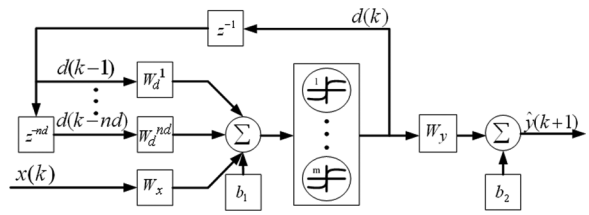

Fig. 8. Globally recurrent neural network architecture.

inputs and outputs of an unknown plant, provide one-step-ahead predictions of the plant outputs. It is assumed that once the model network is capable of generating accurate predictions of the future outputs, it has "learned" the underlying principles governing the dynamic input/output mapping of the plant. The input and output signals specific to the application in this paper are shown in Fig. 10.

The globally recurrent neural network (GRNN) selected in this study is illustrated in Fig. 8 and its output equation is defined in (6). Note the presence of time-delayed feedback loops between the outputs and inputs of the hidden layer. These loops provide the network with memory, and give it the capability to accurately represent arbitrary dynamical systems as demonstrated in [16].

$$\hat{y}(k+1) = f\begin{pmatrix} W_x x(k) + W_d^1 d(k-1) + \\ \vdots \\ W_d^{nd} d(k-nd) + b_1 \end{pmatrix} W_y + b_2 \quad (6)$$

Arguably the most important factor for achieving acceptable performance when using ANNs is the training algorithm. In [17] a discussion of several of the presently available training algorithms is provided, and recommendations are given for the use of conjugate gradient based methods for training ANNs. The gradient calculations follow the truncated back-propagation through time approach outlined in [18].

A C++ based object oriented library implementing ANNs, gradient calculations, and training algorithms is developed for this study. Reference [19] provides some of the concepts needed for such implementations.

B. Model Network Training

GRNN weight updates are limited to offline training, which is completed in the following sequence:

a) Pseudo-random binary signals (PRBSs) are injected to each of the generators in the group at the point labeled u_{LADC} in Fig. 2. Details on how to design appropriate signals for system identification are provided in [20]. Stochastic load changes are applied at multiple locations to ensure the training data contains information about the behavior of the system at different operating points.

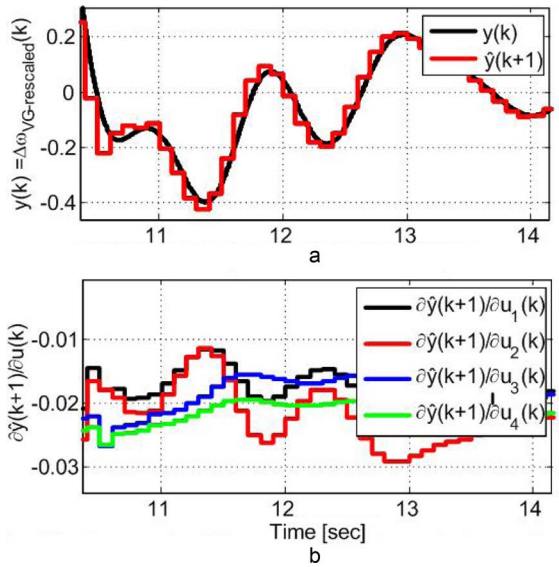

Fig. 9. Model network's one-step-ahead estimate of VG speed and its sensitivity after a 60 ms 3-phase fault at t = 10 s. a- Actual and one-step-ahead estimate of the VG speed; b- sensitivity of one-step-ahead VG speed estimate to changes in the control inputs.

b) 2000 s of input-output pairs (sampled at 10 Hz) are collected as training data and are imported into the C++ neural network library. Some de-trending and scaling of the data is performed to improve learning.
c) The scaled conjugate gradient (SCG) [21] training algorithm generates a set of network weights that minimizes the mean squared error (MSE) over the training data set.

C. Model Network Testing and Sensitivity Estimation

The testing stage ensures that the model network has learned the underlying principles driving the input/output relationship of the plant. PRBSs are no longer applied and disturbances not present in the training set are used instead to excite the system. Accurate predictions of the system output under these conditions are considered an indicator of successful system identification. A typical result observed during testing is shown in Fig. 9(a).

The model network allows the controller adaptation algorithm to estimate the effect of the input signals on the output of the system by providing estimates of the output sensitivities. The ability of NNs to provide accurate estimates of a function and its sensitivities was shown in [22]. The sensitivities are estimated by calculating the partial derivative of the model network's outputs with respect to the network's inputs via backpropagation. Examples these estimates during a disturbance are shown in Fig. 9(b).

V. ILADC Design

The VG identification procedure in the last section provides a differentiable input/output mapping of the dynamical behavior of the VG in the form of a model network. This section describes the implementation of approximate dynamic programming in the form of heuristic dynamic programming (HDP), a mechanism that allows the ILADC to learn and adapt from interactions with the VG and approach optimality as it gains experience. The connections between HDP and classical optimal control can be found in [23]. This type of controller has been shown to outperform other more conventional controllers on a similar application [24].

A. Heuristic Dynamic Programming

Heuristic dynamic programming (HDP) is a reinforcement learning mechanism from the family of adaptive critic designs (ACDs) [25]. In addition to a differentiable model of the system to be controlled, HDP requires two function approximation structures: a critic and an actor. The critic learns to approximate the cost-to-go function in Bellman's equation of dynamic programming, while the actor learns to synthesize the control policy that minimizes the cost-to-go approximated by the critic. The cost-to-go function to be minimized is expressed as:

$$J\left(y(k)\right) = \sum_{i=0}^{\infty} \gamma^i U\left(y(k), u(k)\right) \tag{7}$$

In (7), γ is a scalar discount factor in the $(0 < \gamma < 1)$ interval used for infinite horizon problems, $U(\bullet)$ is a utility function or single-stage cost to be minimized over time that captures the objectives of the control task, and $y(k)$ is the vector of measurements from the plant being controlled.

Both the critic and the actor are implemented using the GRNN shown in Fig. 8. Typically, the plant state vector (not just the plant output vector) is required; however, simulations show that the recurrent nature of the GRNN provides the critic and action networks with internal representations of the state that are good enough for control purposes.

B. Critic Network Training

The key insight that enables the training of the critic in HDP is the recursive form of Bellman's equation (8):

$$J\left(y(k)\right) = U\left(y(k), u(k)\right) + \gamma J\left(y(k+1)\right) \tag{8}$$

HDP progressively adapts the critic network parameters to improve the estimate of (8) by minimizing the following error measure over time [25]:

$$\sum_t \hat{J}\left(y(k)\right) - \left(U\left(y(k), u(k)\right) + \gamma \hat{J}\left(y(k+1)\right)\right) \tag{9}$$

Minimization of (9) can be achieved incrementally by changing the critic network parameters at each time step according to the following weight update rule (10), (11):

$$\Delta w^C(k) = -\eta \left(\hat{J}\left(y(k)\right) - U\left(y(k), u(k)\right) - \gamma \hat{J}\left(\hat{y}(k+1)\right)\right) \frac{\partial \hat{J}\left(y(k)\right)}{\partial w^C(k)} \tag{10}$$

$$w^C\left(k+1\right) = w^C(k) + \Delta w^C(k) \tag{11}$$

where η is a small positive learning rate and w^C is the set of critic GRNN parameters ($W_x, W_d^1, \cdots, W_d^{nd}, b_1, b_2, W_y$ in (6)). The model network developed in the previous section is used to provide the one-step-ahead estimate of the plant output in (10). A slight modification to the critic weight update algorithm similar to strategy 4b in [26] was used to improve the convergence of the critic training procedure. When the error measure in (9) becomes small, the critic is assumed to be capable of providing

an estimate of (7) that is good enough to be used for guiding the adaptation of the action network. This estimate is given by (12).

$$J\left(y(k)\right) \approx \hat{J}\left(\hat{y}(k)\right) \approx U\left(y(k), u(k)\right) + \gamma \hat{J}\left(\hat{y}(k+1)\right) \quad (12)$$

C. Action Network Training

The training of the action network modifies the parameters w^A of the action GRNN ($W_x, W_d^1, \cdots, W_d^{nd}, b_1, b_2, W_y$ in (6)) to improve the performance of the system by minimizing (12). This process begins with calculating an estimate of the sensitivity of the cost-to-go $J(y(k))$ to changes in the system input vector $u(k)$ (13).

$$\frac{\partial J\left(y(k)\right)}{\partial u(k)} \approx \frac{\partial U\left(y(k), u(k)\right)}{\partial u(k)} + \gamma \frac{\partial \hat{y}(k+1)^T}{\partial u(k)} \frac{\partial \hat{J}\left(\hat{y}(k+1)\right)}{\partial \hat{y}(k+1)} \quad (13)$$

This sensitivity can be used to adapt the action network according to the following incremental weight update rule:

$$\Delta w^A(k) = -\eta \frac{\partial \hat{J}\left(y(k)\right)}{\partial w^A(k)} = -\eta \frac{\partial \hat{J}\left(y(k)\right)^T}{\partial u(k)} \frac{\partial u(k)}{\partial w^A(k)} \quad (14)$$

$$w^A(k+1) = w^A(k) + \Delta w^A(k) \quad (15)$$

D. Intelligent Local-Area Damping Controller

The utility function $U(\bullet)$ in (7) must capture the objectives of the control task. For LADC, these objectives reduce to minimizing oscillatory behavior with minimal control effort. By trial and error and following recommendations for utility function design in [27], this function was chosen as (16). The constants C_{CE} and C_{DI} are chosen to achieve an acceptable tradeoff between control effort and damping improvement.

$$U\left(y(k), u(k)\right) = \sum_{i=1}^{N} \left(C_{CE} u_{LADC}^{Gi}(k)^2\right) + C_{DI}\left(\omega_{VG}(k) - 0.4\omega_{VG}(k-1) - 0.3\omega_{VG}(k-2)\right)^2 \quad (16)$$

The complete ILADC configuration incorporating the VG and HDP is illustrated in Fig. 10. The controller adaptation algorithm proceeds in the following order:

a) The action network receives the plant output ω_{VG} and uses it to generate the u_{LADC} signal for the AVR at each of the generators in the coherent group.
b) The model network is used to estimate the effect of these control signals on the future value of ω_{VG} and to calculate its sensitivity to changes in u_{LADC}.
c) The critic network uses the predicted ω_{VG} to estimate the future value of J and its sensitivity to changes in ω_{VG}.
d) If the critic network is undergoing adaptation, (10), (11) are used to improve the weights of the critic network.
e) If the action network is undergoing adaptation, (14), (15) are used to improve the weights of the action network.
f) These steps are repeated at each sampling interval.

Training of the critic and action networks is completed for 1000 s of simulation. At the end of this period the magnitudes of (9) and (13) are small enough to indicate convergence. During training, large random load disturbances at multiple buses in NE and NY disturb the system and cause oscillations of the local area that the action network learns to damp out. These load disturbances also cause significant changes in the steady state power flows, pushing the controller to become robust by learning to perform well at multiple operating points.

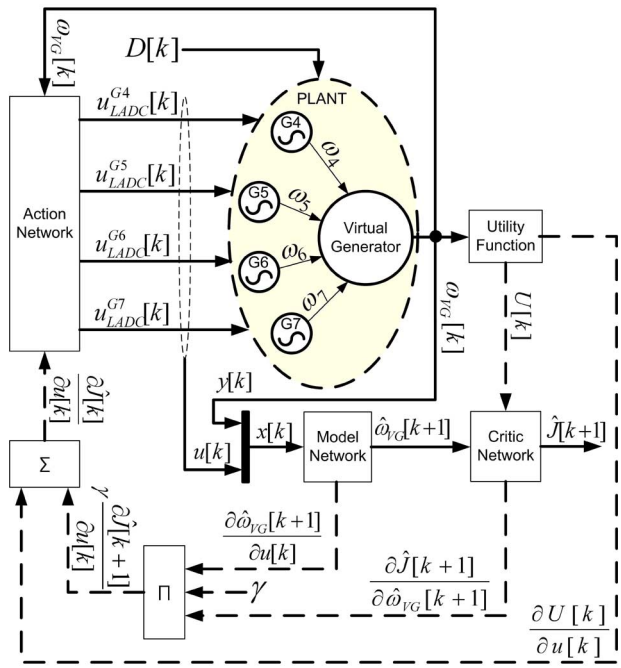

Fig. 10. Combining a VG with HDP to form the ILADC.

VI. Simulation Results

The simulation results shown in this section focus on evaluating the ability of the ILADC to damp low-frequency oscillations resulting from a variety of disturbances applied at different system operating conditions. The disturbances applied and the ILADC connections to the system are shown in Fig. 11. Comparisons are drawn between three different cases: no stabilizing controls (Base), PSS4B-type PSSs (PSS4B), and system with one ILADC (ILADC). PSSs were added to generators G4, G5, G6, and G7 in the second case. The PSS4B parameters for setting 2 in [28] were used for this case. The NN parameters are provided in the Appendix.

Fig. 12 shows the eigenvalues obtained from small signal analysis of the base case system before and after disturbances D2 and D3 in Fig. 11 occur. Only eigenvalues around the frequency range typically associated with electromechanical oscillations (0.1–3 Hz) are shown [29]. The diagonal lines define the set of 5% and 10% damping ratio points. Modes 1–6 show fairly low damping ratios (less than 5–10%), but they are more local in nature, can be expected to decay fairly quickly, and are not particularly sensitive to changes in the operating condition. Modes 7 and 8 show low damping and are inter-area in nature. Mode 8 in particular will decay slowly when the system gets stressed and needs to be addressed. Mode 8 is also highly sensitive to the system's operating condition as demonstrated by its drastic move towards the right of the plane as the NE-NY interconnection is weakened and as the power interchange increases. The right eigenvectors associated with these modes (calculated at t = 129) are used to analyze the mode shapes. Table I summarizes the results. Generators G4–G7 are found to have high participation in the more critical and sensitive mode 8, and some

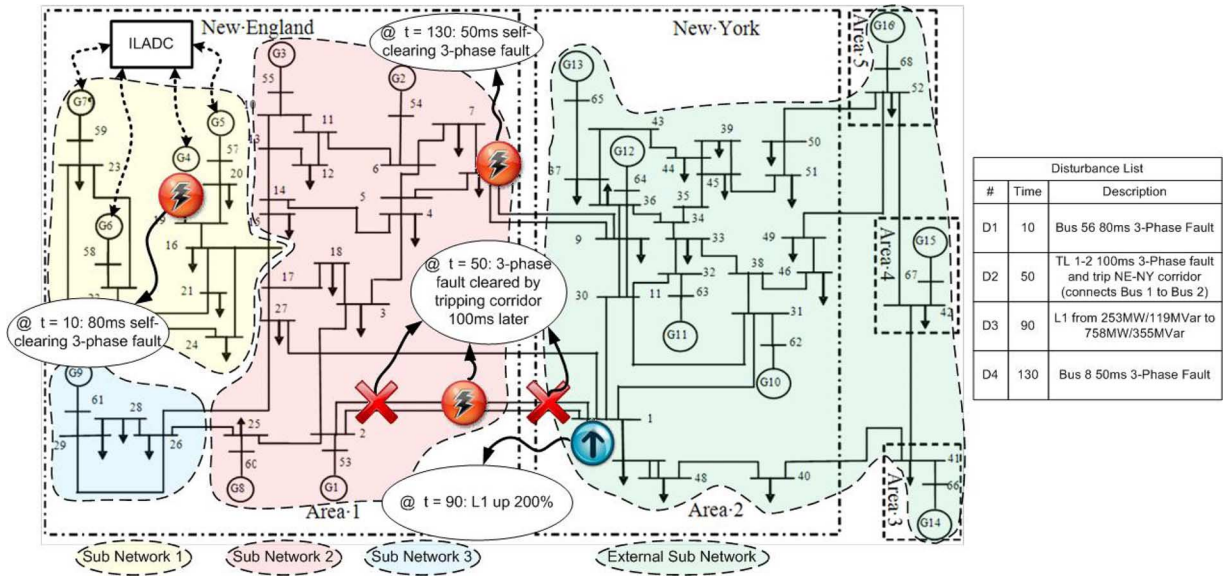

Fig. 11. ILADC connections to system and disturbance times and locations.

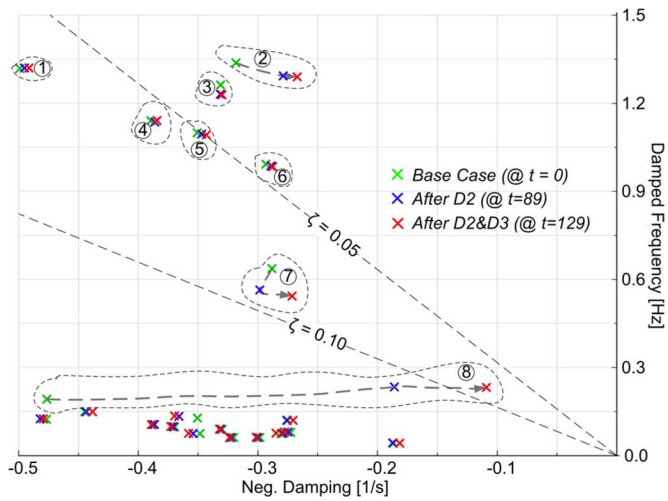

Fig. 12. Eigenvalues of the base case system at different points in the simulation.

TABLE I
SUMMARY OF MODAL ANALYSIS RESULTS

#	Eigenvalues	Freq [Hz]	Damp Ratio [%]	Gens Involved
1	-0.492±j8.294	1.320	5.92	G2 vs. G3
2	-0.267±j8.103	1.290	3.30	G10 vs. Rest
3	-0.330±j7.721	1.229	4.27	G1,G8 vs. Rest
4	-0.385±j7.168	1.141	5.34	G12 vs. Rest
5	-0.343±j6.867	1.092	4.99	G2-G3 vs. G4-G7
6	-0.288±j6.182	0.983	4.65	G9 vs. Rest
7	-0.272±j3.415	0.544	7.93	G10-G13 vs. G4-G9
8	-0.109±j1.456	0.232	7.47	G1-G9 vs. G10-G13

participation in mode 7, indicating that appropriate damping signals at these 4 generators can be effective for damping both of those modes.

The non-linear simulations presented next evaluate the dynamic behavior of the system for the set of disturbances illustrated in Fig. 11 for three different initial load flows. It is known that low-frequency electromechanical oscillations emerge or worsen when large blocks of power are transmitted between distant areas connected by weak tie lines. Therefore, the load flow is varied such that there is a progressive increase in the active power flow from NE to NY. These load flow variations evaluate the capabilities of the different controllers to improve dynamic stability as the system gets pushed closer to its stability limits. Only certain time periods of each simulation are shown due to space limitations.

Figs. 13–17 show the following signals (from top to bottom): rotor speed of generator G4, damping signal injected at generator G4, G4's rotor angle with respect to G13's (slack generator), and active/reactive power exports from NE to NY. In each case, the speed and control input waveforms for generators G5, G6, and G7 are almost identical to those of G4.

The first set of simulations is completed using load flow A, which is characterized by a 720 MW export from NE to NY. Fig. 13 clearly shows the stability improvement provided by both of the damping controllers compared to the uncontrolled base case. The poorly damped low-frequency oscillations present in the base case corresponding to modes 7 and 8 are properly damped for all disturbances. Although not shown, similar results are observed for all other disturbances in Fig. 11. Clearly there is no improvement resulting from the ILADC. This shows that, when properly designed, conventional stabilizing technology can be robust to some changes in the power system dynamics.

The second set of simulations is completed using load flow B, which is characterized by a 974 MW export from NE to NY. The additional generation in NE is distributed equally (in per unit) among all the generators in that area. Active power balance is

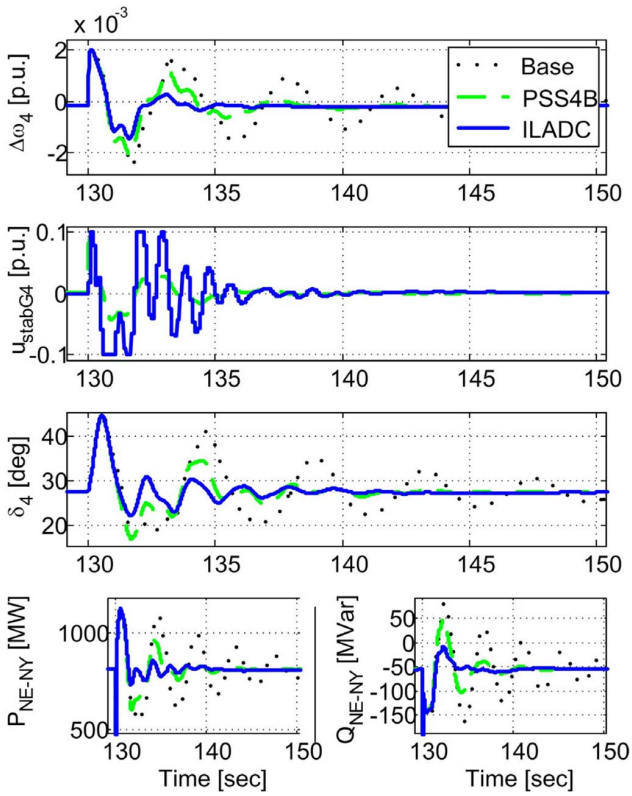

Fig. 13. Results for self-clearing three-phase fault with a weakened interconnection for load flow A.

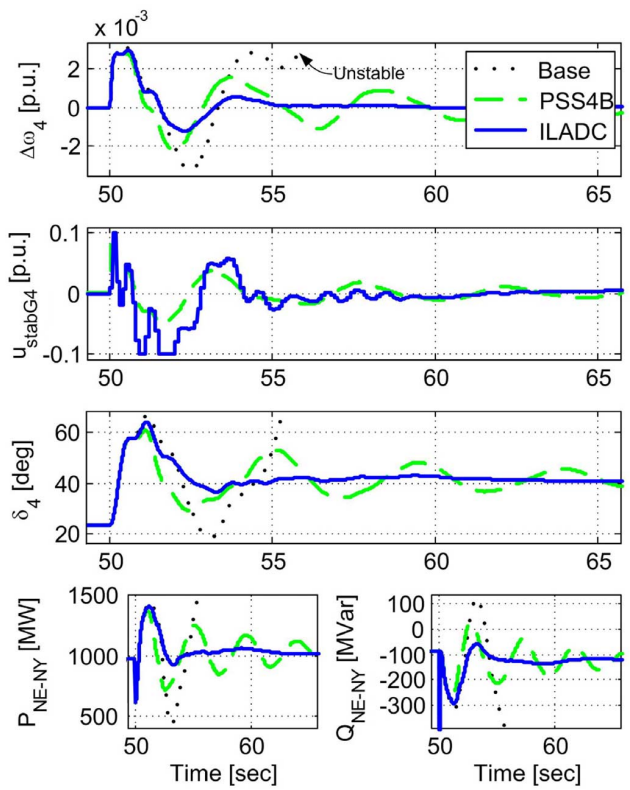

Fig. 14. Results for three-phase fault cleared by tripping an important transmission corridor between NE and NY for load flow B.

achieved by reducing the output of G13 while maintaining all loads unchanged.

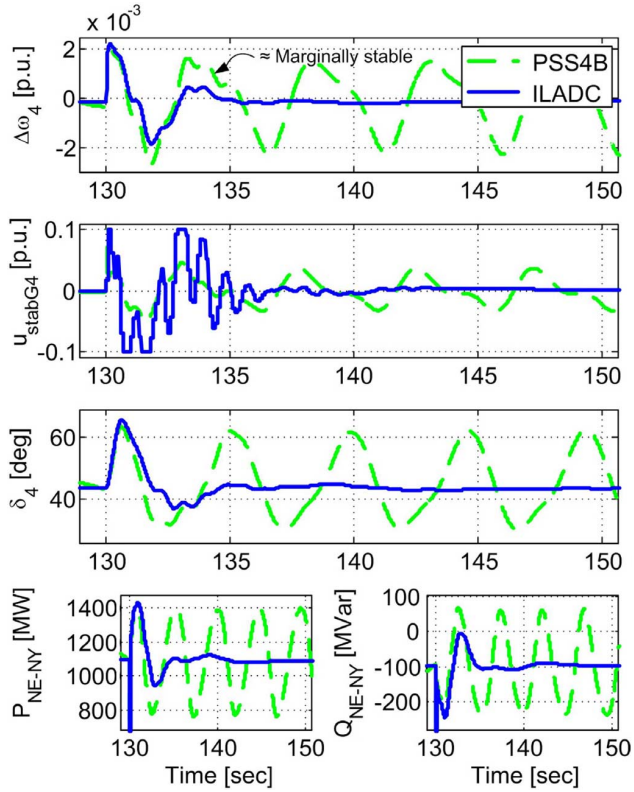

Fig. 15. Results for self-clearing three-phase fault with a weakened interconnection for load flow B.

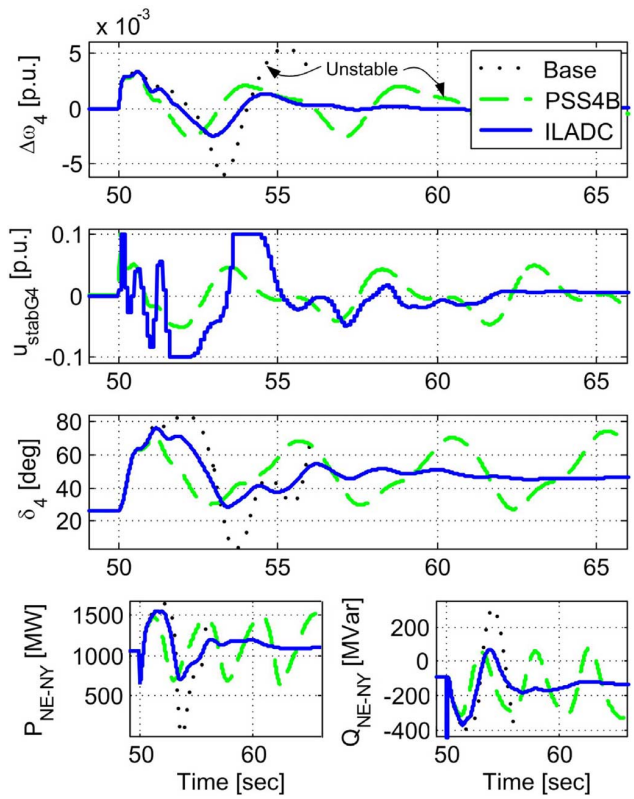

Fig. 16. Results for three-phase fault cleared by tripping an important transmission corridor between NE and NY for load flow C.

Fig. 14 shows that the uncontrolled base case becomes unstable after a three-phase fault is cleared by tripping an important transmission corridor between NE and NY at $t = 50$ (D2 in Fig. 11). The PSS4B case is beginning to show poorly damped

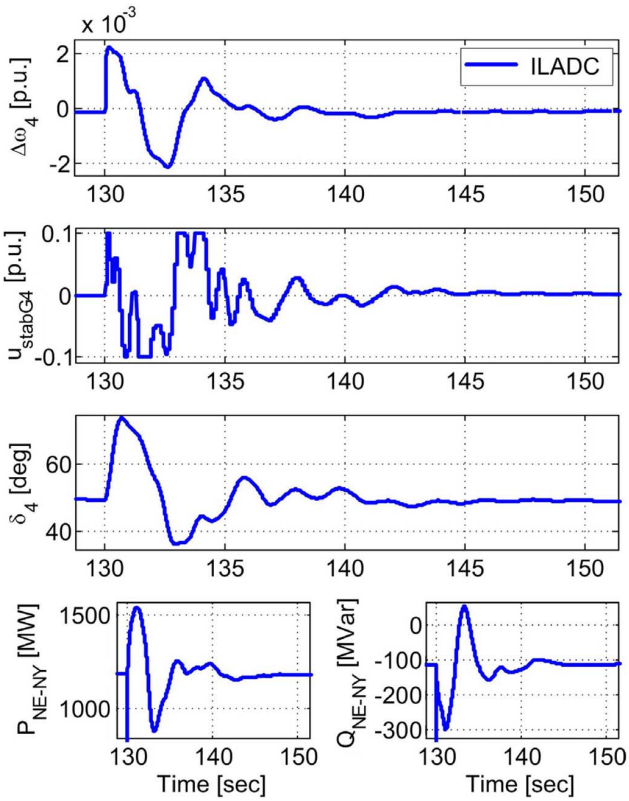

Fig. 17. Results for self-clearing three-phase fault with a weakened interconnection for load flow C.

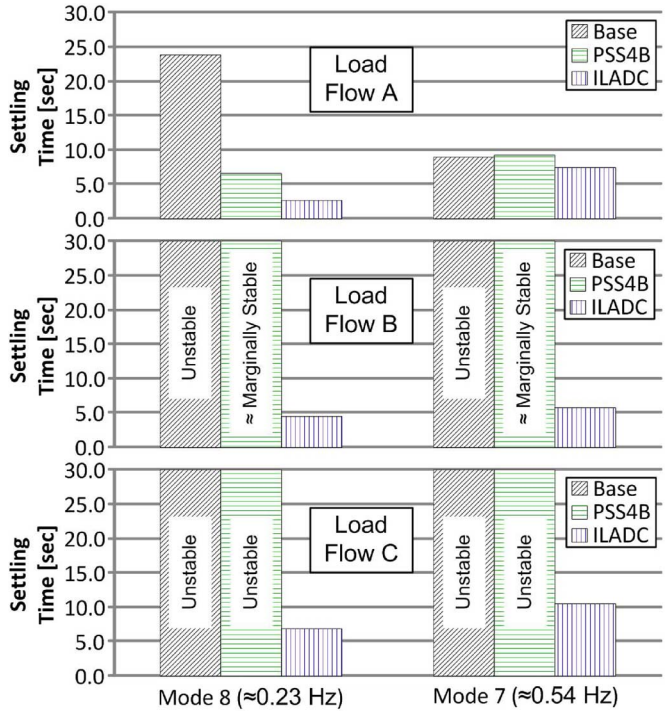

Fig. 18. Settling time estimates for modes 7 and 8 at each load flow with a 10% criterion (time to decay to 10% of initial amplitude).

low-frequency oscillations, indicating that the performance of the PSS4Bs is degrading. In contrast, these oscillations are well damped in the ILADC case in spite of very similar control effort.

Fig. 15 shows that once the system gets pushed further by a load increase at $t = 90$ and disturbed by a self-clearing fault at $t = 130$, the PSS4Bs fail to provide appropriate damping signals and sustained low-frequency oscillations emerge. The additional damping provided by the ILADC allows the system to maintain normal operation. This demonstrates the ILADC improvements over conventional control approaches.

A third set of simulations is carried out using load flow C, which is characterized by a 1053 MW export from NE to NY. Fig. 16 shows that once again the base case system becomes unstable after the events at $t = 50$. This time the PSS4Bs fail to maintain stability and the ILADC's superiority in damping the low-frequency oscillations becomes obvious.

Fig. 17 illustrates how the ILADC is able to cope with the load increase at $t = 90$, and provides appropriate damping even under this heavily loaded operating condition with a weakened NE-NY interconnection. Simulations not presented here show that pushing the system further results in non-oscillatory instability for which the type of controls studied in this paper would be ineffective.

The visual results in Figs. 13–17 are further confirmed by Prony analysis using the Prony Toolbox for MATLAB available in [30]. G4's rotor angle after the last disturbance ($t = 131$–160 time period sampled at 10 Hz) was analyzed. Fig. 18 provides the estimates of the settling times for the dominant low-frequency modes (modes 7 and 8). These plots further confirm that, while the conventional controllers offer acceptable performance for load flow A, once the system gets pushed closer to its limits the performance of those controllers degrades to the point that they can no longer prevent instability. In contrast, the performance degradation of the ILADC is much more gradual and the system remains stable and performs better for a wider range of operation conditions.

These results demonstrate the ability of the ILADC to enhance the operation of the system by enabling power flows that would otherwise result in unstable operation when the system is controlled by more conventional stabilizing technology. Plots of the damping signals at the output of the ILADC illustrate that these enhancements can be achieved with low control effort if the damping signals injected into the system are appropriately generated.

VII. ILADC Implementation Issues, Perspectives, and Potential Solutions

The simulations in the previous section justify further research and development of the ILADC. However, there are practical issues that must be addressed prior to pursuing the use of ILADCs in real power systems. This section briefly discusses some of those issues and offers perspectives and potential solutions.

A. Need for Rotor Angles/Speeds

The VG speed calculation defined by (4) and (5) requires rotor speed measurements. Modern day PMU technology typically measures electrical variables at busses in the system, so these mechanical measurements are likely to be unavailable. However, algorithms for estimating generator speeds using electrical variables have been developed [31], [32]. Also, PMUs capable of measuring rotor speeds [33] may become more common if their use is justified by effective applications.

In a real power system it is unlikely that PMU data from all generators in a coherent group would be available. However, the

VG speed in a large group of machines will be dominated by a few machines with high inertia. These machines will be located at large generating stations that would have priority when measurement networks are installed. An accurate estimate of the VG speed could be obtained using these measurements only.

B. Coherent Groups Can Change

In Section III the effect of the location of an impulse-type disturbance (a fault) on coherency was illustrated. The effects of these types of variations decays quickly and do not have a major impact on the performance of the ILADC. Semi-permanent structural changes of the system (e.g., disconnection of an important transmission line) could completely change the generator clusters. This would have a much more negative and persistent effect on the performance of the ILADC. Thankfully, there are methodologies that can provide coherency based clustering results that are applicable over a wide set of operating conditions/structural configurations [34], [35].

C. Effect of Signal Delays/Signal Loss

It takes a finite amount of time for a signal to travel from a PMU to the ILADC and from the ILADC to the AVR of a generator in local-area. These communication delays can have a negative impact on the performance of the ILADC. However, note that one of the factors that strongly affect coherent behavior is the strength of the interconnection among generators. The stronger the connection, the more likely two generators are to behave coherently. Strong connections typically imply geographical closeness. Therefore, the distance, and by consequence the delay, are likely to be smaller with the ILADC than with other wide-area damping control approaches.

D. Unstable Local Oscillations

The VG calculation essentially "filters out" oscillations inside of the local-area. Some of these oscillations could be unstable and may need damping control. The ILADC cannot "see" such oscillations, and so it is incapable of damping them. However, the ILADC can work with conventional PSSs known to be effective for damping local oscillations. Therefore, these situations would not prevent the use of the ILADC.

VIII. Conclusions

The work in this paper demonstrated the design and evaluation of an intelligent local area signals based damping controller (ILADC) for damping electromechanical oscillations in power systems. Simulations show that the proposed ILADC can damp low-frequency oscillations more effectively than conventional PSSs, enabling increased power transfers that would not be permitted otherwise due to stability constraints. These improvements can be achieved without additional control effort and without affecting the steady state operating conditions of the system. The use of virtual generators makes the proposed ILADC more scalable than the intelligent damping controllers currently available in the literature. This makes the ILADC more feasible for implementation in real systems. However, certain difficulties, some of which are outlined in the paper, must be addressed to ensure feasibility and appropriate performance in real world applications. Current research efforts include evaluating the ILADC on a realistically sized system. The design and effects of multiple ILADC are currently being developed.

Appendix I

GRNN Parameters

Network	Model	Critic	Action
Hidden neurons	10	5	5
Number of delays	3	5	1
Activation function	tansig	tansig	tansig
Sampling frequency	10 Hz	10 Hz	10 Hz
Number of inputs	5	1	1
Number of outputs	1	1	4

Acknowledgment

The authors would like to thank the feedback provided by the reviewers and the editor. Their insightful comments greatly improved the original version of this manuscript.

References

[1] M. Jonson, M. Begovic, and J. Daalder, "A new method suitable for real-time generator coherency determination," *IEEE Trans. Power Syst.*, vol. 19, no. 3, pp. 1473–1482, Aug. 2004.

[2] P. Sauer and M. Pai, *Power System Dynamics and Stability*. Upper Saddle River, NJ: Prentice-Hall, 1998.

[3] M. Aboul-Ela, A. Sallam, J. McCalley, and A. Fouad, "Damping controller design for power system oscillations using global signals," *IEEE Trans. Power Syst.*, vol. 11, no. 2, pp. 767–773, May 1996.

[4] I. Kamwa, A. Heniche, G. Trudel, M. Dobrescu, R. Grondin, and D. Lefebvre, "Assessing the technical value of FACTS-based wide-area damping control loops," in *Proc. 2005 IEEE PESGM*, San Francisco, CA, USA.

[5] I. Kamwa, R. Grondin, and Y. Hebert, "Wide-area measurement based stabilizing control of large power systems—A descentralized/hierarchical approach," *IEEE Trans. Power Syst.*, vol. 16, no. 1, pp. 136–153, Feb. 2001.

[6] Y. Zang and A. Bose, "Design of wide-area damping controllers for interarea oscillations," *IEEE Trans. Power Syst.*, vol. 23, no. 3, pp. 1136–1143, Aug. 2008.

[7] S. Mohagheghi, G. Venayagamoorthy, and R. Harley, "Optimal wide area controller and state predictor for a power system," *IEEE Trans. Power Syst.*, vol. 22, no. 2, pp. 693–705, May 2007.

[8] D. Molina, J. Liang, G. Venayagamoorthy, and R. Harley, "Comparison of TDNN and RNN performances for neuro-identification on small to medium-sized power systems," in *Proc. IEEE CIASG*, Paris, France, 2011.

[9] D. Molina, J. Liang, G. K. Venayagamoorhty, and R. G. Harley, "Virtual generators: Simplified online power system representations for wide-area damping control," in *Proc. IEEE PESGM*, San Diego, CA, USA, 2012.

[10] D. Molina, R. G. Harley, G. K. Venayagamoorthy, D. Falcao, G. N. Taranto, and T. M. L. Assis, "Coherency based partitioning of a power system for intelligent wide-area damping control," in *Proc. 12th SEPOPE*, Rio de Janeiro, Brazil, 2012.

[11] G. Rogers, *Power System Oscillations*. Norwell, MA: Kluwer, 2000.

[12] R. Podmore, "Identification of coherent generators for dynamic equivalents," *IEEE Trans. Power App. Syst.*, vol. PAS-97, no. 4, pp. 1344–1354, Jul./Aug. 1978.

[13] A. Germond and R. Podmore, "Dynamic aggregation of generating unit models," *IEEE Trans. Power App. Syst.*, vol. PAS-97, no. 4, pp. 1060–1069, Jul./Aug. 1978.

[14] J. Chow, R. Galarza, P. Accari, and W. Price, "Inertial and slow coherency aggregation algorithms for power system dynamic model reduction," *IEEE Trans. Power Syst.*, vol. 10, no. 2, pp. 680–685, May 1995.

[15] K. S. Narendra and K. Parthasarathy, "Identification and control of dynamical systems using neural networks," *IEEE Trans. Neural Netw.*, vol. 1, no. 1, pp. 4–27, Mar. 1990.

[16] L. Jin, P. Nikiforuk, and M. Gupta, "Approximation of discrete-time state-space trajectories using dynamic recurrent neural networks," *IEEE Trans. Autom. Control*, vol. 40, no. 7, pp. 1266–1270, Jul. 1995.

[17] T. Masters, *Advanced Algorithms for Neural Networks: A C++ Sourcebook*. London, U.K.: Academic, 1995.

[18] D. Prokhorov, G. Puskorius, and L. Feldkamp, "Dynamical neural networks for control," in *A Field Guide to Dynamical Recurrent Networks*, J. Kolen and S. Kremer, Eds. New York: IEEE Press, 2001.
[19] J. Rogers, *Object-Oriented Neural Networks in C++*. London, U.K.: Academic, 1997.
[20] Y. Zhu, *Multivariable System Identification for Process Control*. Oxford, U.K.: Elsevier, 2010.
[21] M. F. Moller, "A scaled conjugate gradient algorithm for fast supervised learning," *Neural Netw.*, vol. 6, no. 4, pp. 525–533, 1993.
[22] H. White and A. Gallant, "On learning the derivatives of an unknown mapping with multilayer feedforward networks," *Neural Netw.*, vol. 5, pp. 129–138, 1992.
[23] S. Ferrari and R. F. Stengel, "Model-based adaptive critic designs," in *Handbook of Learning and Approximate Dynamic Programming*, J. Si, A. Barto, W. Powell, and D. Wunsch, Eds. New York: Wiley, Jul. 2004.
[24] S. Ray, G. Venayagamoorthy, B. Chaudhuri, and R. Majumder, "Comparison of adaptive critic-based and classical wide-area controllers for power systems," *IEEE Trans. Syst., Man, Cybern. B, Cybern.*, vol. 38, no. 4, pp. 1002–1007, Aug. 2008.
[25] D. Prokhorov and D. Wunsch, "Adaptive critic designs," *IEEE Trans. Neural Netw.*, vol. 8, no. 5, pp. 997–1007, Sep. 1997.
[26] G. G. Lendaris and C. Paintz, "Training strategies for critic and action neural networks in dual heuristic dynamic programming method," in *Proc. ICNN*, Houston, TX, USA, 1997, vol. 2, pp. 712–717.
[27] G. K. Venayagamoorthy, R. G. Harley, and D. C. Wunsch, "Dual heuristic programming excitation neurocontrol for generators in a multimachine power system," *IEEE Trans. Ind. Appl.*, vol. 39, no. 2, pp. 382–394, 2003.
[28] I. Kamwa, R. Grondin, and G. Trudel, "IEEE PSS2B versus PSS4B: The limits of performance of modern power system stabilizers," *IEEE Trans. Power Syst.*, vol. 20, no. 2, pp. 903–915, 2005.
[29] P. Kundur, *Power System Stability and Control*. New York: McGraw-Hill, 1993.
[30] S. Singh and J. C. Hamann, Prony Toolbox [Online]. Available: http://www.mathworks.com/matlabcentral/fileexchange/3955 last accessed on Aug. 29, 2012
[31] A. Angel, P. Geurts, D. Ernst, M. Glavic, and L. Wehenkel, "Estimation of rotor angles of synchronous machines using artificial neural networks and local PMU-based quantities," *Neurocomputing*, vol. 70, pp. 2668–2678, 2007.
[32] E. Chahremani and I. Kamwa, "Online state estimation of a synchronous generator using unscented Kalman filter from phazor measurement units," *IEEE Trans. Energy Convers.*, vol. 26, no. 4, pp. 1099–1108, 2011.
[33] Q. Yang, T. Bi, and J. Wu, "WAMS implementation in China and the challenges for bulk power system protection," in *Proc. IEEE PESGM*, 2007.
[34] I. Kamwa, A. K. Pradhan, and G. Joos, "Automatic segmentation of large power system into fuzzy coherent areas for dynamic vulnerability assessment," *IEEE Trans. Power Syst.*, vol. 22, no. 4, pp. 1974–1985, 2007.
[35] I. Kamwa, A. K. Pradhan, G. Joos, and S. R. Samantaray, "Fuzzy partitioning of a real power system for dynamic vulnerability assessment," *IEEE Trans. Power Syst.*, vol. 24, no. 3, pp. 1356–1365, 2009.

Diogenes Molina (S'07) received the B.S.E.E. degree from John Brown University, Siloam Springs, AR, USA, in 2007 and the M.S.E.E. degree from the University of Arkansas, Fayetteville, AR, USA, in 2009. He is currently working toward the Ph.D. degree in electrical engineering from the Georgia Institute of Technology, Atlanta, GA, USA.

His research interests include the development of intelligent algorithms for optimization and control of power systems, power system simulations, optimal home energy management, motor drives, and other grid connected power electronics.

Ganesh Kumar Venayagamoorthy (S'91–M'97–SM'02) received the Ph.D. degree in electrical engineering from the University of Natal, Durban, South Africa, in 2002.

He is the Duke Energy Distinguished Professor of Electrical and Computer Engineering at Clemson University, Clemson, SC, USA. Prior to that, he was a Professor of Electrical and Computer Engineering at the Missouri University of Science and Technology (Missouri S&T), Rolla, MO, USA. He was a Visiting Researcher with ABB Corporate Research, Sweden, in 2007. He is Founder and Director of the Real-Time Power and Intelligent Systems Laboratory (http://rtpis.org). His research interests are in the development and applications of advanced computational algorithms for smart grid applications, including power system stability and control, optimization, operations, signal processing, intelligent sensing, monitoring and control. He has published 2 edited books, 8 book chapters, and over 90 refereed journals papers and 300 refereed conference proceeding papers.

Dr. Venayagamoorthy is a recipient of several awards including the 2010 Innovation Award from St. Louis Academy of Science, and the 2010 IEEE Region 5 Outstanding Member Award. He is the recipient of the 2012 Institution of Engineering and Technology (IET) Generation, Transmission and Distribution Premier Award for the best research paper published during last two years for the paper "Wide area control for improving stability of a power system with plug-in electric vehicles." He is involved in the leadership and organization of many conferences including the co-Chair of the 2013 IEEE Symposium of Computational Intelligence Applications in Smart Grid (CIASG) to be held in Singapore. He is currently the Chair of the IEEE PES Working Group on Intelligent Control Systems, and the Founder and Chair of IEEE Computational Intelligence Society (CIS) Task Force on Smart Grid. He is currently an Editor of the IEEE TRANSACTIONS ON SMART GRID. He is a Fellow of the IET, U.K., and the SAIEE.

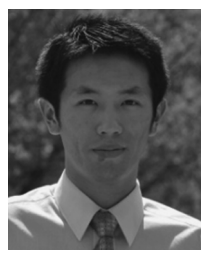

Jiaqi Liang (S'08–M'12) received the B.Eng. degree in electrical engineering from Tsinghua University, Beijing, China, in 2007, and the M.S. and Ph.D. degrees in electrical engineering from the Georgia Institute of Technology, Atlanta, GA, USA, in 2009 and 2012, respectively.

He is currently a Research Scientist with the ABB US Corporate Research Center, Raleigh, NC, USA. His research interests include electric machines and their drive systems, power electronics converters, HVDC and FACTS, renewable energy grid integration, and power system control and operation.

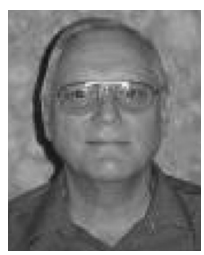

Ronald G. Harley (M'77–SM'86–F'92) received the Ph.D. degree from London University, London, U.K., in 1969.

He is currently a Regents' Professor and the Duke Power Company Distinguished Professor at the Georgia Institute of Technology, Atlanta, GA, USA. His research interests include the dynamic behavior of electric machines, motor drives, power systems and their components, wind and solar energy, and controlling them by the use of power electronics and intelligent control algorithms. He has coauthored some 500 papers in refereed journals and international conferences and five patents.

Dr. Harley received in 2005 The Cyril Veinott Electromechanical Energy Conversion Award from the IEEE Power Engineering Society for "Outstanding contributions to the field of electromechanical energy conversion," and in 2009 the IEEE Richard H. Kaufmann field award with citation "For contributions to monitoring, control and optimization of electrical processes including electrical machines and power networks."